The Journal of Physiological Sciences (2019) 69:199–209
https://doi.org/10.1007/s12576-018-0635-3

ORIGINAL PAPER

Intracellular Ca^{2+} mobilization pathway via bradykinin B_1 receptor activation in rat trigeminal ganglion neurons

Reiko Terashima[1,2] · Maki Kimura[2] · Asuka Higashikawa[2] · Yuki Kojima[2] · Tatsuya Ichinohe[1] · Masakazu Tazaki[2] · Yoshiyuki Shibukawa[2]

Received: 5 February 2018 / Accepted: 20 August 2018 / Published online: 4 September 2018

Abstract

Bradykinin (BK) and its receptors, B_1 and B_2, in trigeminal ganglion (TG) neurons are involved in the regulation of pain. Recent studies have revealed that B_1 receptors are expressed in neonatal rat TG neurons; however, the intracellular signaling pathway following B_1 receptor activation remains to be elucidated. To investigate the mechanism by which B_1 receptor activation leads to intracellular Ca^{2+} mobilization, we measured the intracellular free Ca^{2+} concentration ($[Ca^{2+}]_i$) in primary-cultured TG neurons. The application of Lys-[Des-Arg^9]BK (B_1 receptor agonist) increased the $[Ca^{2+}]_i$ in these TG neurons even in the absence of extracellular Ca^{2+}. Pretreatment with inhibitors of ryanodine receptors or sarco/endoplasmic reticulum Ca^{2+}-ATPase suppressed the increase in Lys-[Des-Arg^9]BK-induced $[Ca^{2+}]_i$. The Lys-[Des-Arg^9]BK-induced $[Ca^{2+}]_i$ increase was unaffected by phospholipase-C inhibitor. B_1 receptor activation-induced $[Ca^{2+}]_i$ increase was suppressed by phosphodiesterase inhibitor and enhanced by adenylyl cyclase inhibitor. These results suggest that B_1 receptor activation suppresses intracellular cAMP production via adenylyl cyclase inhibition and mobilizes intracellular Ca^{2+} via ryanodine receptors that access intracellular Ca^{2+} stores.

Keywords Adenylyl cyclase · Ca^{2+} mobilization · Cyclic AMP · G protein · Ryanodine receptors · Trigeminal ganglion neuron

Introduction

Bradykinin (BK) and related peptides play important roles in the modulation of physiological and pathological processes, including pain and inflammation [1]. The kallikrein–kinin system comprises kininogens, proteolytic kallikrein enzymes, BK and Lys-BK (kallidin; produced through the cleavage of kininogens by kallikreins), [Des-Arg^9]BK and Lys[Des-Arg^9]BK (produced through the cleavage of BK and kallidin, respectively) and BK receptors [2]. Both BK and Lys-BK are vasoactive peptides synthesized by the kallikrein–kinin system. Their metabolites without the C-terminal arginine residue act as ligands of BK receptors [1]. The BK receptors localized to the plasma membrane belong to the G protein-coupled receptor (GPCR) family and are classified into two subtypes, B_1 and B_2. It has been shown that BK itself activates B_2 receptors [1] and that BK has a 100- to 20,000-fold higher affinity for B_2 receptors than for B_1 receptors [1]. Both Lys-BK and Lys[Des-Arg^9]BK have higher affinities for B_1 receptors than do BK and [Des-Arg^9]BK, respectively. The only natural kinin sequence with a subnanomolar affinity for B_1 receptors is Lys[Des-Arg^9]BK [1]. For mammalian BK receptors, the order of agonist affinity is: Lys[Des-Arg^9]BK > Lys-BK ≈ [Des-Arg^9]BK » BK for B_1 receptors; BK ≈ Lys-BK » [Des-Arg^9]BK » Lys[Des-Arg^9]BK for B_2 receptors [1]. Thus, the agonist showing the highest affinity for B_1 receptors is Lys[Des-Arg^9]BK, with much higher affinities than BK itself.

Neuropathic pain, which is mediated by both B_1 and B_2 receptor activation in the orofacial area, is often induced by injuries to trigeminal ganglion (TG) neurons or glial cells [2–4]. B_1 receptors have been suggested as an attractive target for the control of neuropathic pain [2]. In a previous study [3], we demonstrated functional expression of B_1 and B_2 receptors in TG neurons, observing that BK elicited

✉ Yoshiyuki Shibukawa
yshibuka@tdc.ac.jp

[1] Department of Dental Anesthesiology, Tokyo Dental College, Tokyo 101-0061, Japan

[2] Department of Physiology, Tokyo Dental College, Tokyo 101-0061, Japan

increases in intracellular free Ca^{2+} concentration ($[Ca^{2+}]_i$) that were inhibited by B_2 receptor antagonists, but not by B_1 receptor antagonists, whereas application of Lys-[Des-Arg^9]BK induced increases in $[Ca^{2+}]_i$ that were sensitive to a B_1 receptor antagonist. We therefore concluded that B_1 receptors in TG neurons, similar to those elsewhere in the brain, show high selectivity for Lys-[Des-Arg^9]BK [3]. In addition, the activation of B_2 receptors induced both the influx of Ca^{2+} from the extracellular medium and the release of Ca^{2+} from intracellular Ca^{2+} stores [3]. However, the intracellular signaling pathway by which Lys-[Des-Arg^9]BK induces Ca^{2+} mobilization in response to the activation of B_1 receptors had not yet been fully elucidated.

Intracellular Ca^{2+} is mobilized by two closely coupled components: Ca^{2+} entry from the extracellular space and the release of Ca^{2+} from intracellular stores. Ca^{2+} release from intracellular stores is mediated by inositol 1,4,5-trisphosphate (IP_3) receptors or ryanodine receptors. Ligand binding to the GPCR leads to phospholipase C (PLC) activation that in turn induces the production of IP_3 and subsequent IP_3-induced Ca^{2+} release. Ryanodine receptors are known to elicit Ca^{2+}-induced Ca^{2+} release following depolarization-induced Ca^{2+} entry and/or Ca^{2+} release via IP_3 receptors.

In the study reported here, we measured $[Ca^{2+}]_i$ in primary-cultured rat TG neurons and used various agonists and antagonists to investigate the intracellular signaling pathway that is activated by the administration of Lys-[Des-Arg^9]BK.

Materials and methods

Ethical approval

All animals were treated in accordance with the Guiding Principles for the Care and Use of Animals in the Field of Physiological Science approved by the Council of the Physiological Society of Japan, and the American Physiological Society. This study also followed the guidelines established by the U.S. National Institutes of Health (Bethesda, MD, USA) on the care and use of animals for experimental procedures. The study was approved by the Ethics Committee of Tokyo Dental College (Approval no. 292503).

Isolation of trigeminal ganglion cells

Trigeminal ganglion cells were isolated from neonatal Wistar rats (7–8 days old) under pentobarbital sodium anesthesia (50 mg/kg), following the administration of isoflurane (3.0% vol). TG cells were dissociated by enzymatic treatment with Hanks' balanced salt solution (137 mM NaCl, 5.0 mM KCl, 2.0 mM $CaCl_2$, 0.5 mM $MgCl_2$, 0.44 mM KH_2PO_4, 0.34 mM Na_2HPO_4, 4.17 mM $NaHCO_3$, 5.55 mM glucose) containing 20 U/ml papain (Worthington, Lakewood, NJ, USA) for 20 min at 37 °C, followed by dissociation by trituration. After dissociation, the TG cells were plated on 35-mm diameter dishes (ibidi GmbH, Planegg, Germany). The primary culture of the TG cells was performed in Leibovitz's L-15 medium (Life Technologies, Carlsbad, CA, USA), containing 10% fetal bovine serum, 1% amphotericin B, 1% fungizone (Life Technologies), 26 mM $NaHCO_3$ and 30 mM glucose (pH 7.4). The cells were maintained in culture for 48 h at 37 °C in a humidified atmosphere containing 95% oxygen and 5% CO_2 to allow cell attachment to the bottom of dishes. For measurement of $[Ca^{2+}]_i$, the temperature of the extracellular medium was maintained at 32 °C (Warner Instruments, Hamden, CT, USA) to avoid thermal stimulation of cells.

Solutions and reagents

Hanks' balanced salt solution was used as the standard extracellular solution. A solution containing a high concentration of extracellular K^+ (91 mM NaCl, 50 mM KCl, 2.0 mM $CaCl_2$, 0.5 mM $MgCl_2$, 0.44 mM KH_2PO_4, 0.34 mM Na_2HPO_4, 4.17 mM $NaHCO_3$, 5.55 mM glucose; pH 7.4) was used to distinguish TG neurons from glial cells through activation of depolarization-induced increases in $[Ca^{2+}]_i$ in the neurons. The endogenous potent and highly selective bradykinin B_1 receptor agonist Lys-[Des-Arg^9]BK [3], the sarco/endoplasmic reticulum Ca^{2+}-ATPase (SERCA) inhibitor cyclopiazonic acid (CPA, 100 nM [5]), the ryanodine receptor inhibitor dantrolene (sodium salt, 1 μM [5, 6]), the phosphodiesterase (PDE) inhibitor isobutylmethylxanthine (IBMX, 50 μM [5]), the phospholipase C inhibitor U73122 (100 nM [7]) and the adenylyl cyclase inhibitor SQ22536 (1 μM [5, 8]) were obtained from Tocris Bioscience (Bristol, UK). Xestospongin C [9], which antagonizes the calcium-releasing action of IP_3 at the receptor level without interacting with the IP_3-binding site, was purchased from Wako Pure Chemical Industries, Ltd. (Osaka, Japan). All other reagents were purchased from Sigma Chemical Co. (St. Louis, MO, USA), except where indicated.

Measurement of the $[Ca^{2+}]_i$ concentration

Primary-cultured TG cells were loaded with 10 μM fura-2 acetoxymethyl ester (DOJINDO, Kumamoto, Japan) and 0.1% (w/v) pluronic F-127 acid (Life Technologies) in Hanks' solution (90 min at 37 °C, 5% CO_2). The cultured TG cells were then rinsed with fresh Hanks' solution. A dish containing fura-2-loaded TG cells was mounted onto the stage of a microscope (model IX73; Olympus Corp., Tokyo, Japan) equipped with HCImage software, an excitation wavelength selector and an intensified charge-coupled device camera system (Hamamatsu Photonics, Hamamatsu, Japan). Fura-2 fluorescence emissions were recorded at

510 nm under alternating excitation wavelengths of 380 nm (F380) and 340 nm (F340). The $[Ca^{2+}]_i$ was measured as the fluorescence ratio of F340 and F380 ($R_{F340/F380}$), expressed in F/F_0 units; that is, the $R_{F340/F380}$ value (F) was normalized to the resting value (F_0). The F/F_0 baseline was set at 1.0. We evaluated $[Ca^{2+}]_i$ responses as changes in the F/F_0 values using the formula:

$$\text{Change in fluorescence } (\Delta F) = F \big/ F_{0peak} - F \big/ F_{0base},$$

where F/F_{0peak} was the value obtained at peak $[Ca^{2+}]_i$ response; F/F_{0base} indicates the value just before the application of certain pharmacological agents.

Statistical and offline analysis

The data are expressed as the mean ± standard error of the mean of N observations, where N represents the number of independent experiments or cells. The Wilcoxon rank-sum test, Kruskal–Wallis test or Mann–Whitney U test were used to determine nonparametric statistical significance. A p value of < 0.05 was considered to be significant. Statistical analysis was performed using GraphPad Prism 5.0 (GraphPad Software Inc., La Jolla, CA, USA).

Results

Lys-[Des-Arg^9]BK, a B_1 receptor agonist, induced $[Ca^{2+}]_i$ increases in TG neurons

Primary-cultured TG neurons exhibited a round-shaped cell body that ranged in diameter from 7.2 to 53.6 µm (Fig. 1a). We first examined the response of these neurons to Lys-[Des-Arg^9]BK-induced $[Ca^{2+}]_i$ in both the presence and absence of external Ca^{2+}. In the presence of extracellular Ca^{2+} (2.0 mM), the first application of Lys-[Des-Arg^9]BK (10 nM) evoked transient increases in $[Ca^{2+}]_i$ to peak values of 0.61 ± 0.07 ΔF units, and the second application of this molecule evoked transient increases in $[Ca^{2+}]_i$ to peak values of 0.54 ± 0.07 ΔF units (Fig. 1b, c). Following the removal of Ca^{2+} from the extracellular solution, repeated addition of Lys-[Des-Arg^9]BK (10 nM) again produced rapid and transient increases in $[Ca^{2+}]_i$, reaching peak values of 0.18 ± 0.05 ΔF units for the first application, and 0.11 ± 0.02 ΔF units for the second application (Fig. 1b, c). There was no significant difference in the peak values between the first and second applications of Lys-[Des-Arg^9]BK in either the presence or absence of extracellular Ca^{2+} (Fig. 1c). However, there were significant differences in the amplitudes of the Lys-[Des-Arg^9]BK-induced $[Ca^{2+}]_i$ increases as a function of the presence or absence of extracellular Ca^{2+} (Fig. 1c). After extracellular Ca^{2+} was restored to the extracellular solution, the baseline level of $[Ca^{2+}]_i$ increased, and Lys-[Des-Arg^9]BK-induced $[Ca^{2+}]_i$ increases could also be observed (Fig. 1b, c). Irrespective of cell body diameter (Fig. 1a), 119 of 127 neurons (from 16 experiments) responded to Lys-[Des-Arg^9]BK.

Effects of inhibition of ryanodine receptors and SERCAs

Following repeated application of Lys-[Des-Arg^9]BK, the addition of the SERCA inhibitor CPA (100 nM) gradually increased $[Ca^{2+}]_i$ in both the presence (Fig. 2a) and absence (Fig. 2c) of extracellular Ca^{2+}. After the CPA-induced $[Ca^{2+}]_i$ increase reached a plateau, subsequent application of Lys-[Des-Arg^9]BK resulted in a further increase in $[Ca^{2+}]_i$ (Fig. 2a) in the presence of extracellular Ca^{2+}, but only quite small $[Ca^{2+}]_i$ increases occurred in the absence of extracellular Ca^{2+} (Fig. 2c). In both the presence (Fig. 2b) and absence (Fig. 2d) of extracellular Ca^{2+}, the ΔF values of the $[Ca^{2+}]_i$ increases induced by Lys-[Des-Arg^9]BK in the presence of 100 nM CPA were significantly smaller than those induced in the absence of CPA.

The ryanodine receptor inhibitor dantrolene (1.0 µM dantrolene sodium salt) significantly abolished Lys-[Des-Arg^9]BK-induced $[Ca^{2+}]_i$ increases, reducing them to ΔF values of 0.10 ± 0.02 and 0.20 ± 0.03 in the absence (Fig. 3a, b) and presence (Fig. 3c, d), respectively, of external Ca^{2+}. Notably, the Lys-[Des-Arg^9]BK-induced $[Ca^{2+}]_i$ increases were observed after Ca^{2+} was restored to the extracellular medium following Ca^{2+}-free conditions (Fig. 3a).

Effects of PLC inhibition

To examine the effects of PLC or IP_3 receptor inhibition, we first measured the increase in Lys-[Des-Arg^9]BK-elicited $[Ca^{2+}]_i$ in the absence of extracellular Ca^{2+} (Fig. 4a). We then restored extracellular Ca^{2+} and allowed the $[Ca^{2+}]_i$ to reach a steady state, following which we once again observed increases in Lys-[Des-Arg^9]BK-induced $[Ca^{2+}]_i$. When we applied the PLC inhibitor U73122 (100 nM) in the absence of extracellular Ca^{2+}, the baseline value of $[Ca^{2+}]_i$ further gradually increased. In the presence of U73122 but absence of extracellular Ca^{2+}, Lys-[Des-Arg^9]BK again increased the $[Ca^{2+}]_i$. We did not observe any significant effect of the presence or absence of U73122 on the ΔF values resulting from the application of Lys-[Des-Arg^9]BK in the absence of extracellular Ca^{2+} (Fig. 4a, b).

In addition, application of xestospongin C (1 µM [9]) did not show any effects on the Lys-[Des-Arg^9]BK-induced $[Ca^{2+}]_i$ increases in the presence of extracellular Ca^{2+} (Fig. 4c, d).

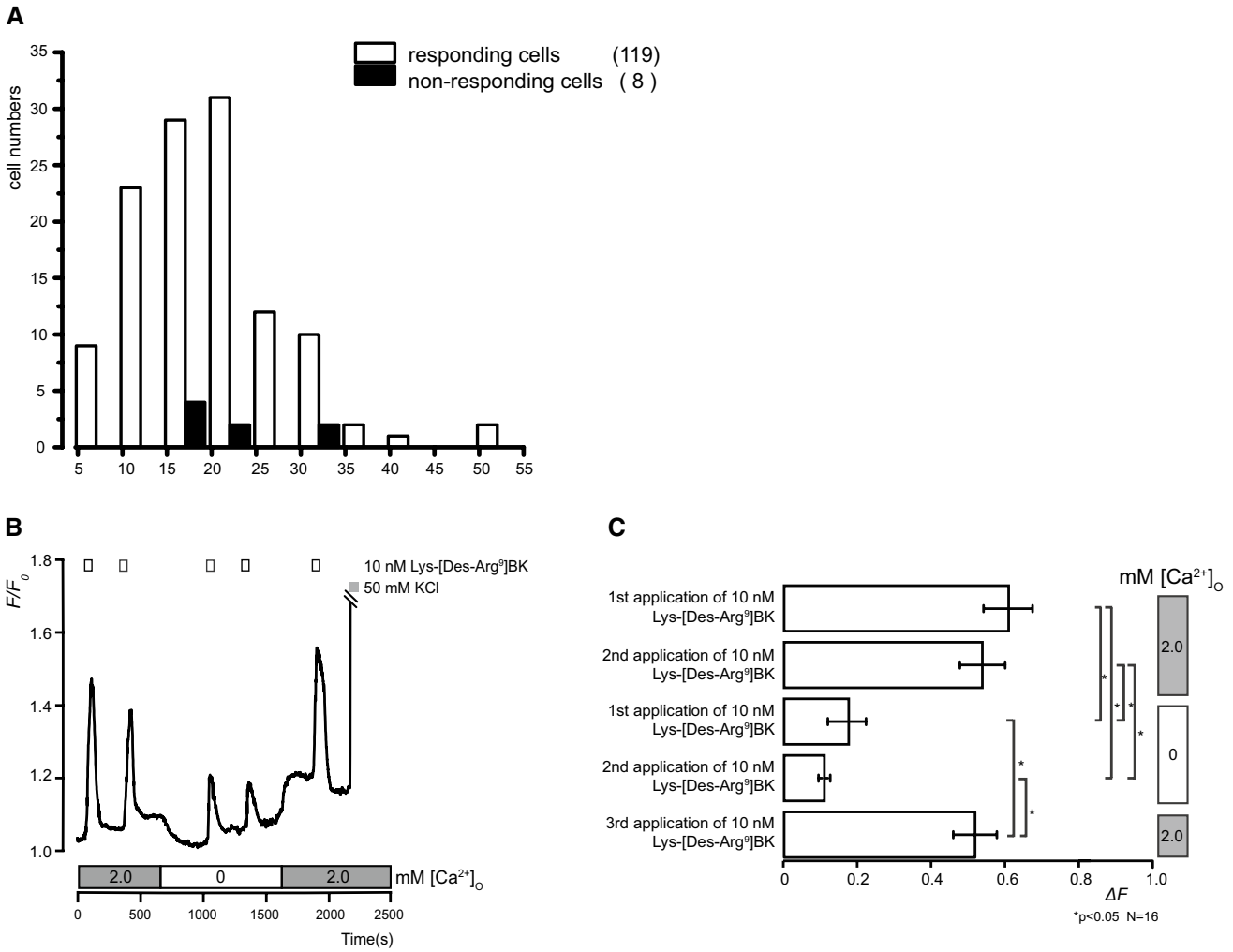

Fig. 1 Range in diameter of primary-cultured trigeminal ganglion (TG) cells and increases in the intracellular free Ca^{2+} concentration ($[Ca^{2+}]_i$) in primary-cultured TG neurons following the application of Lys-[Des-Arg^9]BK, a B_1 receptor agonist. **a** Distribution of the cell body diameter of Lys-[Des-Arg^9]BK-responding (white segment of bars) and -non-responding TG neurons (black segment of bars) are shown for 127 neurons in total (from 16 experiments). **b** Example of transient $[Ca^{2+}]_i$ increases following the application of 10 nM Lys-[Des-Arg^9]BK (white boxes at top of graph) in the presence (gray segments of lower horizontal bar) or absence (white segment of lower horizontal bar) of extracellular Ca^{2+} (2.0 mM). Gray square on the upper-right side of graph indicates the timing of an application of a high-extracellular-K^+ (50 mM) solution. **c** Summary bar graph showing $[Ca^{2+}]_i$ increases following applications of 10 nM Lys-[Des-Arg^9]BK. Upper, second from the top, and lowermost bar show the values following the first, second and third application of 10 nM Lys-[Des-Arg^9]BK, respectively, in the presence of external Ca^{2+} (2.0 mM) (gray boxes on right side of graph). Third and fourth bar from the top show the mean values for the increase in $[Ca^{2+}]_i$ following the first and second application of 10 nM Lys-[Des-Arg^9]BK, respectively, in the absence of external Ca^{2+} (white box on the right side of graph). Each bar denotes the mean ± standard error (SE) of 16 experiments. Statistical significance between bars (shown by solid lines) is indicated by asterisks: $*p < 0.05$

Effects of intracellular cAMP increases and adenylyl cyclase inhibition

In the presence of extracellular Ca^{2+}, repeated application of Lys-[Des-Arg^9]BK elicited $[Ca^{2+}]_i$ increases (Figs. 5a, 6a). IBMX (50 μM), a selective PDE inhibitor that raises intracellular cAMP levels, significantly and reversibly inhibited the increases in $[Ca^{2+}]_i$ induced by Lys-[Des-Arg^9]BK (Fig. 5a, b). Conversely, SQ22536 (0.1 μM), an adenylyl cyclase inhibitor that decreases intracellular cAMP levels, significantly enhanced the increases in $[Ca^{2+}]_i$ induced by Lys-[Des-Arg^9]BK in the presence of extracellular Ca^{2+} (Fig. 6a, b).

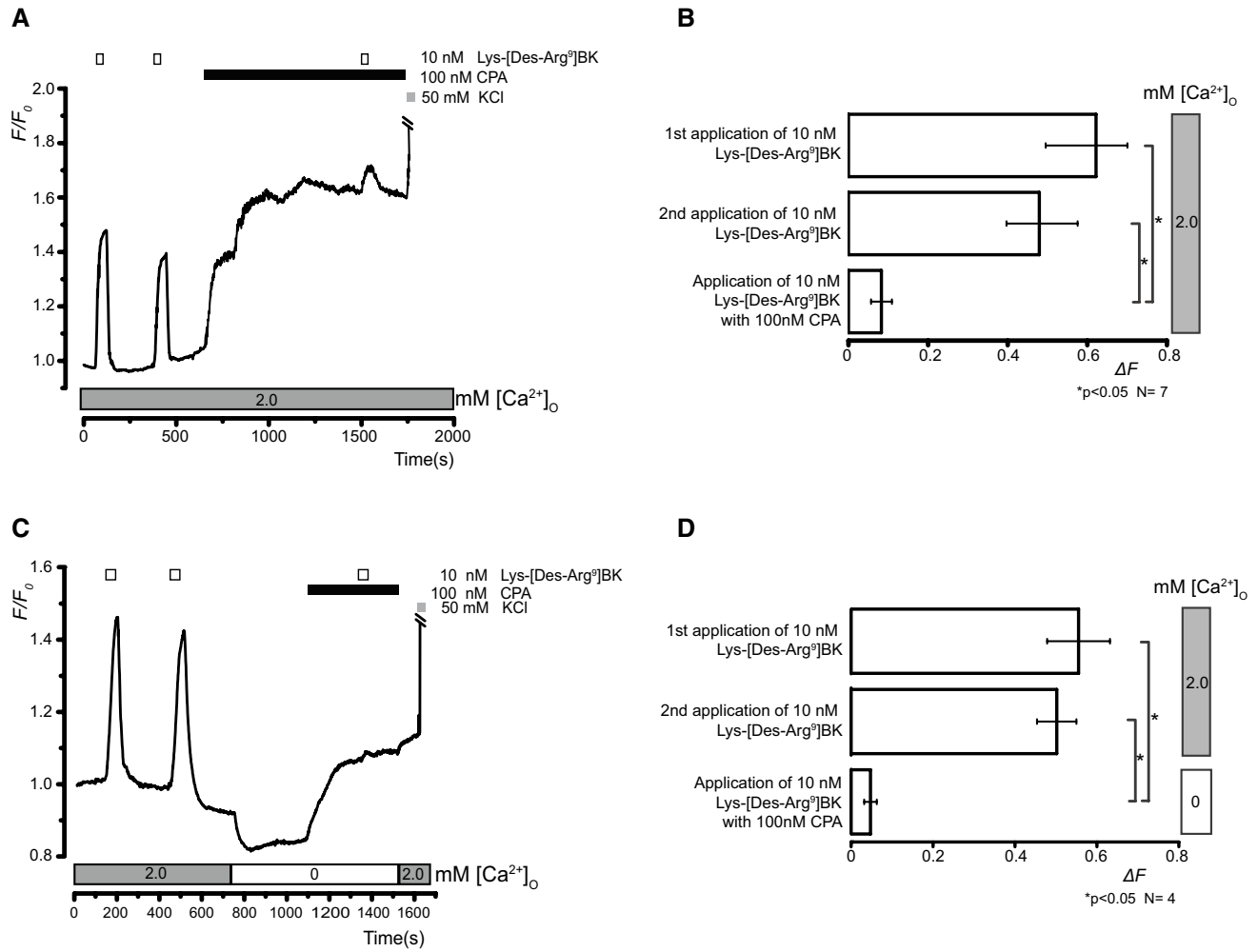

Fig. 2 Effects of sarcoplasmic reticulum Ca^{2+}-ATPase inhibitors on $[Ca^{2+}]_i$. **a** Representative $[Ca^{2+}]_i$ trace upon additions of Lys-[Des-Arg^9]BK (upper white boxes) is shown. Application of 100 nM of cyclopiazonic acid (*CPA*; black bar at top of graph) gradually elicited an increase in $[Ca^{2+}]_i$, and the subsequent application of Lys-[Des-Arg^9]BK (10 nM) induced a further increase in transient $[Ca^{2+}]_i$. **b** Summary bar graph showing $[Ca^{2+}]_i$ increases following the first (upper bar) and second (middle bar) application of 10 nM Lys-[Des-Arg^9]BK in the presence of external Ca^{2+} (2.0 mM) and following the application of 10 nM Lys-[Des-Arg^9]BK with 100 nM CPA (lowermost bar) in the presence of extracellular Ca^{2+} (gray box on the upper-right side of graph). Each bar denotes the mean ± SE of seven experiments. **c** Following the repetitive $[Ca^{2+}]_i$ increases triggered by Lys-[Des-Arg^9]BK (white boxes at top of graph), extracellular Ca^{2+} was removed and 100 nM CPA was applied (black bar at top of graph), which gradually elicited an increase in $[Ca^{2+}]_i$, with the subsequent application of Lys-[Des-Arg^9]BK (10 nM) inducing a considerably small transient $[Ca^{2+}]_i$ increase. Gray boxes on the upper-right side of graphs in **a** and **c** indicates the timing for application of the high extracellular-K^+ (50 mM) solution. **d** Summary bar graph showing $[Ca^{2+}]_i$ increases following the first (upper bar) and second (middle bar) application of 10 nM Lys-[Des-Arg^9]BK in the presence of external Ca^{2+} (2.0 mM) (gray box on the right side of graph) and following the application of 10 nM Lys-[Des-Arg^9]BK with 100 nM CPA (lowermost bar) in the absence of extracellular Ca^{2+} (white box on the right side of graph). Each bar denotes the mean ± SE of the mean of four experiments. Statistical significance between the bars in **b** and **d** (shown by solid lines) is indicated by asterisks: $*p < 0.05$.

Discussion

The results of our study show that B_1 receptor activation by Lys-[Des-Arg^9]BK in TG neurons induced increases in the $[Ca^{2+}]_i$ in both the presence and absence of extracellular Ca^{2+}, thereby indicating that B_1 receptors are capable of mobilizing Ca^{2+} by triggering Ca^{2+} release from intracellular stores. Notably, almost all of the primary-cultured TG neurons (93.7%) responded to Lys-[Des-Arg^9]BK. The distribution of the cell body diameter of TG neurons in the present study is consistent with that reported in our previous study [10]. The amplitudes of the Lys-[Des-Arg^9]BK-induced $[Ca^{2+}]_i$ increases in the absence of extracellular Ca^{2+} were significantly smaller than those in the presence of extracellular Ca^{2+} (Fig. 1), indicating that Lys-[Des-Arg^9]BK mobilizes Ca^{2+} not only by releasing it from intracellular stores, but also by inducing Ca^{2+} influx from the extracellular medium. These results are in agreement with those from

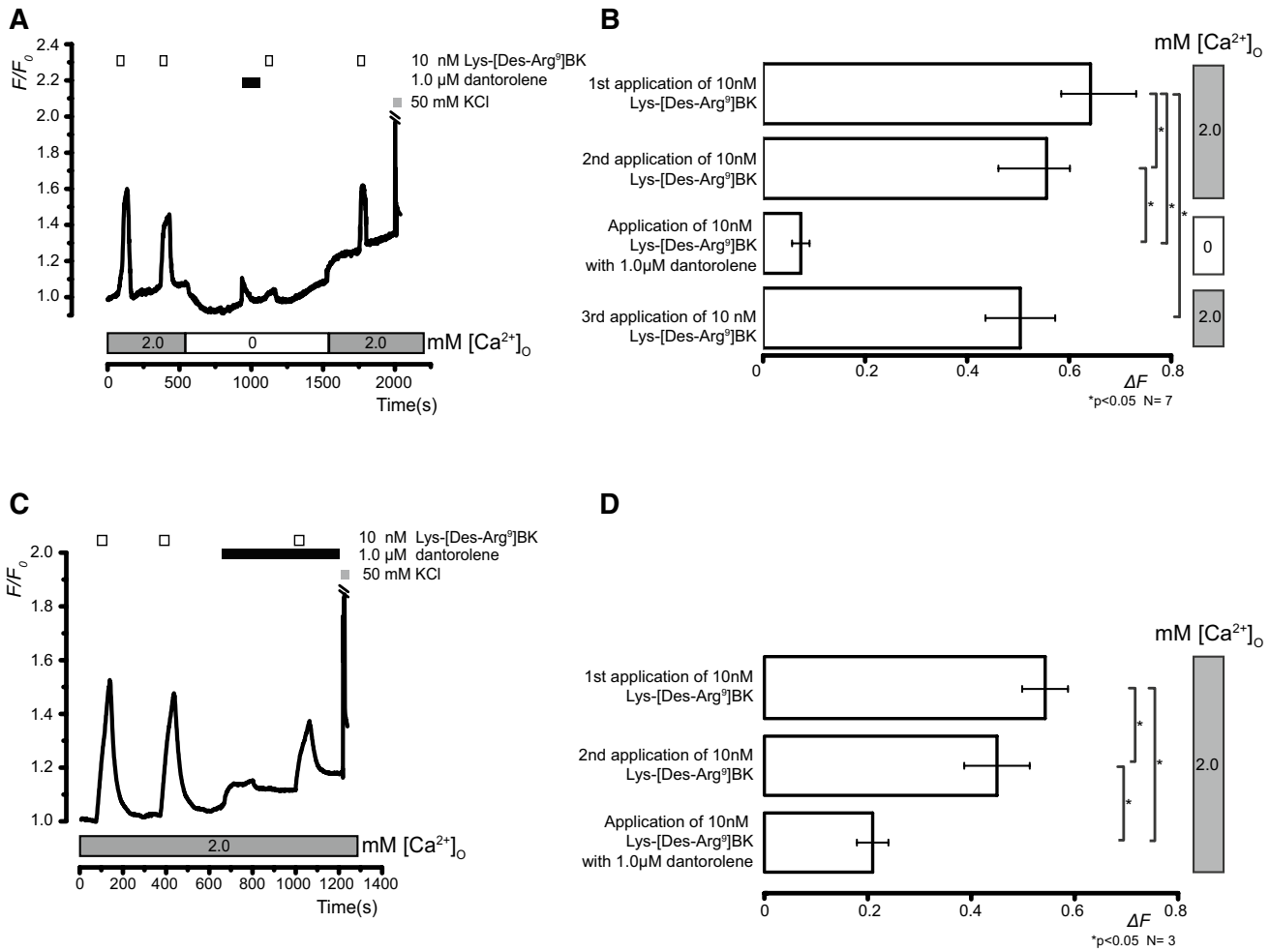

Fig. 3 Effects of ryanodine receptor inhibitors on $[Ca^{2+}]_i$. **a** Representative trace of $[Ca^{2+}]_i$ produced by repeated additions of Lys-[Des-Arg^9]BK (white boxes at top of graph) in the presence (2.0 mM; gray segments of lower bar) or absence of extracellular Ca^{2+} (white segment of lower bar) is shown. The increase in $[Ca^{2+}]_i$ induced by 10 nM Lys-[Des-Arg^9]BK was inhibited by the application of 1.0 μM dantrolene (upper black box) in the absence of external Ca^{2+}. Gray box on the upper-right side of graph indicates the timing of application of the high-extracellular-K^+ (50 mM) solution. **b** Summary bar graph showing $[Ca^{2+}]_i$ increases following the first (upper bar), second (second bar from the top) and third (lowermost bar) application of 10 nM Lys-[Des-Arg^9]BK in the presence of external Ca^{2+} (2.0 mM; gray boxes on right side of graph), and following the application of 10 nM Lys-[Des-Arg^9]BK in the presence of 1.0 μM dantrolene (third bar from the top) in the absence of external Ca^{2+} (white box on the right side of graph). Each bar denotes the mean ± SE of seven experiments. **c** Following the repetitive Lys-[Des-Arg^9]BK-induced $[Ca^{2+}]_i$ increases (upper white boxes) in the presence (2.0 mM: lower gray bar) of extracellular Ca^{2+}, we applied 1.0 μM dantrolene (upper black box). The increase in $[Ca^{2+}]_i$ induced by 10 nM Lys-[Des-Arg^9]BK was inhibited by the application of 1.0 μM dantrolene in the presence of external Ca^{2+}. The gray boxes on the upper-right side of the graphs in **a** and **c** indicate the timing for application of high-extracellular-K^+ (50 mM) solution. **d** Summary bar graph showing the $[Ca^{2+}]_i$ increases following the first (upper bar) and second (middle bar) application of 10 nM Lys-[Des-Arg^9]BK with external Ca^{2+} (2.0 mM; vertical gray bar on the right side of graph), and following the application of 10 nM Lys-[Des-Arg^9]BK with 1.0 μM dantrolene (lowermost bar). Each bar denotes the mean ± SE of the mean of three experiments. In **b** and **d**, the statistical significance between bars (shown by solid lines) is indicated by asterisks: $*p < 0.05$

our previous study showing that B_2 receptor activation in TG neurons also induced both Ca^{2+} release and Ca^{2+} influx [3]. In vascular smooth muscle cells, Mathis et al. observed that B_1 receptor activation not only elevated $[Ca^{2+}]_i$ by inducing the release of Ca^{2+} from intracellular Ca^{2+} stores, but also produced $[Ca^{2+}]_i$ oscillations that were dependent on Ca^{2+} influx from the extracellular medium [11]. In embryonic chick heart cells, El-Bizri et al. observed BK-activated T-type and L-type voltage-dependent Ca^{2+} currents that were partially inhibited by a B_1 receptor antagonist [12]. However, Kitakoga and Kuba reported that in their study BK did not elicit Ca^{2+} currents in TG neurons [13]. Recently, Ifuku et al. demonstrated that microglial migration mediated by the activation of B_1 receptors depends on the Ca^{2+} entry mode (or "reverse mode" producing Ca^{2+} influx) of Na^+/Ca^{2+} exchanger (NCX) activity (NCX-induced Ca^{2+} influx;

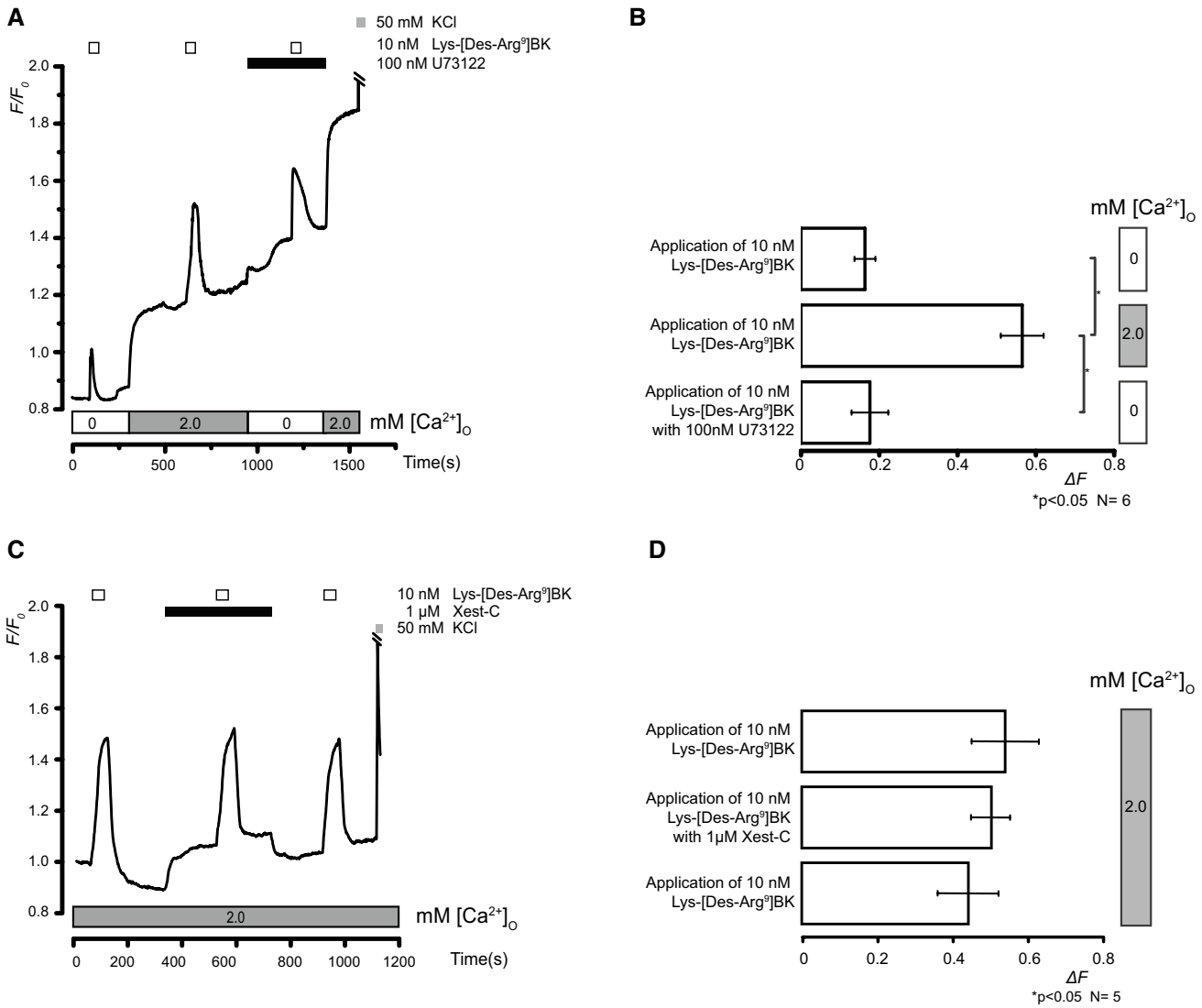

Fig. 4 Inhibition of phospholipase C (PLC) did not affect the increase in $[Ca^{2+}]_i$ induced by Lys-[Des-Arg^9]BK in TG neurons. **a** Representative trace of 10 nM Lys-[Des-Arg^9]BK-induced $[Ca^{2+}]_i$ increases (white boxes at top of graph) in the absence (white segments of lower horizontal bar) or the presence (gray segments of lower horizontal bar) of extracellular Ca^{2+} (2.0 mM). The increase in $[Ca^{2+}]_i$ induced by 10 nM Lys-[Des-Arg^9]BK was not affected by the application of 100 nM U73122 (black bar at top of graph) in the absence of external Ca^{2+}. Gray box on the upper-right side of the graph indicates an application timing of high-extracellular-K^+ (50 mM) solution. **b** Summary bar graph showing $[Ca^{2+}]_i$ increases following the application of 10 nM Lys-[Des-Arg^9]BK (upper and middle bar), and following the application of 10 nM Lys-[Des-Arg^9]BK with 100 nM U73122 (lower bar), with or without external Ca^{2+} (2.0 mM) (gray or white boxes on the right side of graph, respectively). **c** Representative trace of 10 nM Lys-[Des-Arg^9]BK-induced $[Ca^{2+}]_i$ increases (upper white boxes) in the presence (lower gray bar) of extracellular Ca^{2+} (2.0 mM). The increase in $[Ca^{2+}]_i$ induced by 10 nM Lys-[Des-Arg^9]BK was not affected by the application of 1 μM xestospongin C (*Xest-C*; black bar at top of graph). The gray box on the upper-right side of graph indicates the timing for application of high-extracellular-K^+ (50 mM) solution. **d** Summary bar graph showing $[Ca^{2+}]_i$ increases following the application of 10 nM Lys-[Des-Arg^9]BK (upper and lowermost bar) and following the application of 10 nM Lys-[Des-Arg^9]BK with 1 μM xestospongin C (middle bar), with external Ca^{2+} (2.0 mM) (vertical gray bar). Each bar denotes the mean ± SE of six experiments in **b** and five experiments in **d**, respectively. In **b** and **d**, the statistical significance between bars (shown by solid lines) is indicated by asterisks: $*p < 0.05$

[14]). We previously reported the expression of NCX isoforms (NCX1, NCX2, and NCX3) in primary-cultured rat TG neurons and observed reverse mode of NCX activity that was functionally coupled to voltage-dependent Na^+ channels [15]. Although further study will be needed to clarify the extracellular Ca^{2+} influx pathway induced by B_1 receptor activation in TG neurons, the results from our present study show that B_1 receptors mobilized intracellular Ca^{2+} via tryanodine receptors that access intracellular Ca^{2+} stores (see below).

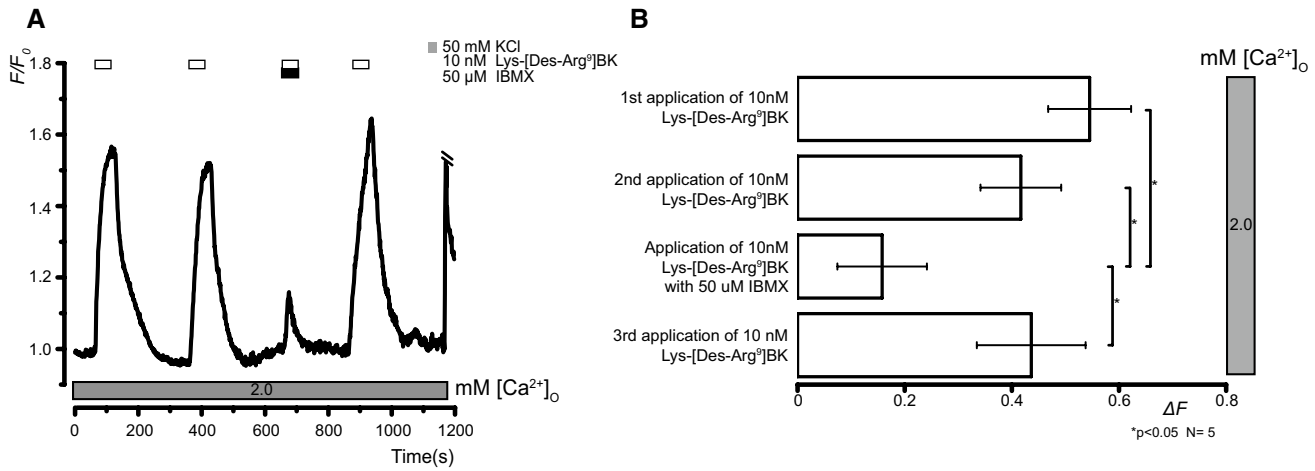

Fig. 5 Intracellular cAMP levels modulate the increase in $[Ca^{2+}]_i$ induced by Lys-[Des-Arg^9]BK in TG neurons. **a** Example of transient increases in $[Ca^{2+}]_i$ during the application of 10 nM Lys-[Des-Arg^9]BK (white boxes at top of graph), with or without 50 μM isobutylmethylxanthine (*IBMX*; upper black box), in the presence of external Ca^{2+} (2.0 mM). Gray box on the upper-right side of graph indicates an application timing of high-extracellular-K^+ (50 mM) solution. **b** Summary bar graph showing $[Ca^{2+}]_i$ increases following the first (upper bar), second (second from the top bar) and third (lowermost bar) application of 10 nM Lys-[Des-Arg^9]BK in the presence of external Ca^{2+} (2.0 mM), and following the application of 10 nM Lys-[Des-Arg^9]BK with 50 μM IBMX (third bar from the top). Each bar denotes the mean ± SE of five experiments. Statistical significance between bars (shown by solid lines) is indicated by asterisks: $*p < 0.05$.

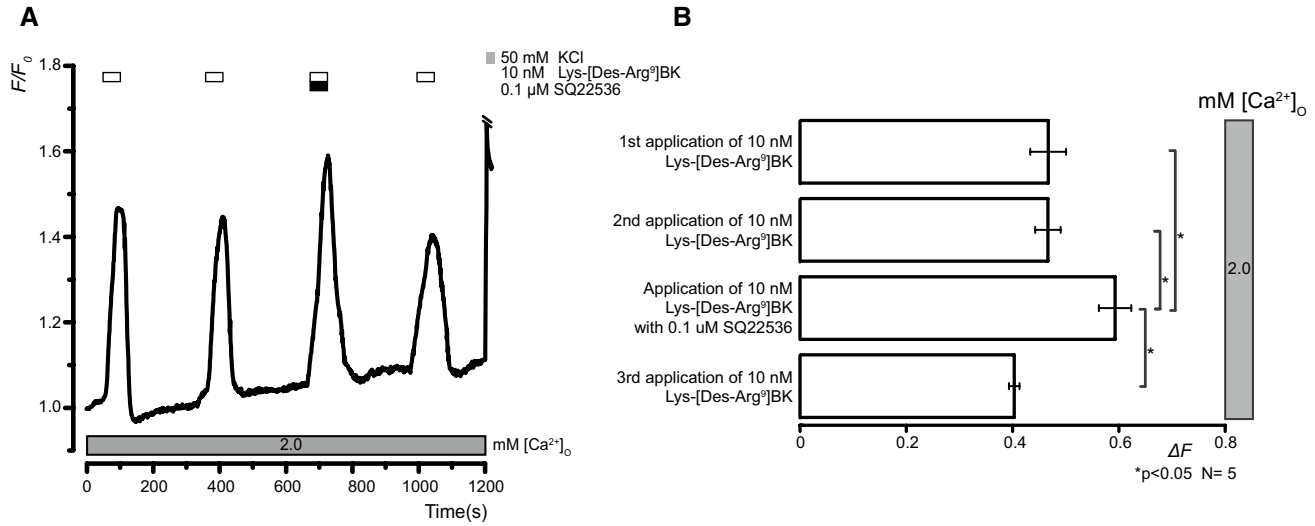

Fig. 6 Inhibition of adenylyl cyclase enhances the increase in $[Ca^{2+}]_i$ induced by Lys-[Des-Arg^9]BK in TG neurons. **a** Example of transient increases in $[Ca^{2+}]_i$ during the application of 10 nM Lys-[Des-Arg^9]BK (upper white boxes), in the presence or absence of 0.1 μM SQ22536 (upper black box), in the presence of external Ca^{2+} (2.0 mM). Gray box on the upper-right side of graph indicates an application timing of high-extracellular-K^+ (50 mM) solution. **b** Summary bar graph showing $[Ca^{2+}]_i$ increases following the first (upper bar), second (second bar from the top) and third (lowermost bar) application of 10 nM Lys-[Des-Arg^9]BK with external Ca^{2+} (2.0 mM), and following the application of 10 nM Lys-[Des-Arg^9]BK with 0.1 μM SQ22536 (third bar from the top). Each bar denotes the mean ± SE of five experiments. Statistical significance between bars (shown by solid lines) is indicated by asterisks: $*p < 0.05$.

We found that a SERCA pump inhibitor, CPA, reduced the ΔF amplitude of B_1 receptor activation-induced $[Ca^{2+}]_i$ increases, while increasing the baseline values of the $[Ca^{2+}]_i$ in both the absence and presence of external Ca^{2+}. This process resulted from both the leakage of Ca^{2+} from the intracellular Ca^{2+} store and the accumulation of $[Ca^{2+}]_i$ by suppression of movement of Ca^{2+} into that store. In the absence of extracellular Ca^{2+}, CPA almost completely abolished the Lys-[Des-Arg^9]BK-induced $[Ca^{2+}]_i$ increases, compared with those in the absence of CPA, suggesting

depletion of the Ca^{2+} that is released from the intracellular stores by B_1 receptor activation. The Lys-[Des-Arg^9]BK-induced Ca^{2+} release in TG neurons in both the absence and presence of extracellular Ca^{2+} was also sensitive to a ryanodine receptor inhibitor. These results indicate that B_1 receptors activate Ca^{2+} release from internal stores via ryanodine receptors.

The B_1 receptor is directly coupled to G proteins of the G_q and G_i families [1]. The B_1 agonist generated by the degradation of BK activates B_1 receptors coupled to the G_q family [1, 14]. Activation of the G_q family mediates the phosphoinositide turnover signaling pathway, resulting in a $[Ca^{2+}]_i$ increase through the generation of IP_3 via activation of PLC. Interestingly, however, administration of not only the PLC inhibitor U73122, but also the membrane-permeable IP_3 receptor blocker xestospongin C did not affect the Lys-[Des-Arg^9]BK-induced Ca^{2+} increases. Thus, these results suggest that the PLC-IP_3 signaling pathway might not contribute to the Lys-[Des-Arg^9]BK-induced Ca^{2+} release from the intracellular stores via ryanodine receptors in the TG neurons. In addition, the subsequent Ca^{2+} release from ryanodine receptors elicited by IP_3-mediated Ca^{2+} release might also be unlikely. In the present study, although dantrolene almost completely suppressed the Lys-[Des-Arg^9]BK-induced Ca^{2+} release in TG neurons, we observed a residual component of the $[Ca^{2+}]_i$ increase during application of dantrolene in both the presence and absence of extracellular Ca^{2+}. Therefore, we cannot exclude the contribution of the PLC-IP_3 signaling cascade to Lys-[Des-Arg^9]BK-induced Ca^{2+} mobilization in TG neurons. However, the Lys-[Des-Arg^9]BK-induced Ca^{2+} mobilization may be mediated by another signaling pathway, such as the cAMP-dependent pathway, rather than a PLC-coupling Gq pathway (see below).

Since both U73122 [16] and xestospongin C [17] exert inhibitory effects on not only the IP_3-mediated Ca^{2+} release but also the SERCA pumps, in our study they increased the baseline F/F_0 value. Therefore, the U73122- and xestospongin C-induced increases in the baseline F/F_0 value resulted from SERCA inhibition. The SERCA inhibitor CPA also increased the baseline F/F_0 value. The presence of CPA almost completely suppressed the Lys-[Des-Arg^9]BK-induced Ca^{2+} increases, while exposure to U73122 and xestospongin C did not affect the increase. These results suggest that U73122 and xestospongin C more efficiently inhibit the PLC–IP_3 signaling pathway than do the SERCA pumps in TG neurons.

In contrast, activation of the G_i family suppresses the production of cAMP from ATP. In the present study, increasing the intracellular cAMP level by applying the selective PDE inhibitor IBMX reduced the amplitude of Lys-[Des-Arg^9]BK-induced $[Ca^{2+}]_i$ increases (PDE hydrolyzes cAMP into inactive 5′-AMP). Decreases in intracellular cAMP levels induced by the inhibition of adenylyl cyclase (by SQ22536) had the opposite effect. These results indicate that B_1 receptor activation increases the $[Ca^{2+}]_i$ by suppressing adenylyl cyclase activity and thereby decreasing intracellular cAMP level. In our recent study, activation of the $P2Y_{12}$ receptor, a G protein-coupled nucleotide receptor expressed in TG neurons, also increased the $[Ca^{2+}]_i$; the $P2Y_{12}$ receptor-induced $[Ca^{2+}]_i$ increase is also sensitive to a ryanodine receptor inhibitor [5]. In addition, in the same study, application of SQ22536 to the primary-cultured TG neurons resulted in a concentration-dependent increase in $[Ca^{2+}]_i$, while the application of IBMX inhibited the $P2Y_{12}$ receptor activation-mediated $[Ca^{2+}]_i$ increase. These results are in agreement with our present results, showing that, in the TG neurons, a decrease in intracellular cAMP levels due to the suppression of adenylyl cyclase following the activation of B_1 receptor increases the $[Ca^{2+}]_i$, thereby suggesting that intracellular Ca^{2+} mobilization by Lys-[Des-Arg^9]BK may possibly be regulated by a cAMP-dependent G_i pathway.

It has been demonstrated that activation of cAMP-dependent protein kinase (protein kinase A) results in inhibition of PLC activity, IP_3 production and subsequent IP_3-induced Ca^{2+} mobilization during smooth muscle relaxation [18, 19], implying that a reduction of cAMP production is capable of enhancing IP_3-induced Ca^{2+} release. The results of our present study show that the PLC inhibitor and IP_3 receptor blocker did not have any effect on the Lys-[Des-Arg^9]BK-induced Ca^{2+} increases in TG neurons, while the reduction of cAMP levels by B_1 receptor activation triggered an increase in the $[Ca^{2+}]_i$ via ryanodine receptors. Taken together, our results suggest that intracellular Ca^{2+} mobilization may possibly be regulated by a cAMP-dependent G_i pathway, but not by PLC activity or IP_3-induced Ca^{2+} release. Further studies are needed to clarify the detailed mechanism of cAMP-dependent Ca^{2+} release via ryanodine receptors, following activation of not only B_1 receptors but also $P2Y_{12}$ receptors.

The expression of B_1 receptors is induced rapidly in response to tissue damage or inflammation [20]. This expression pattern of B_1 receptors suggests that they may play a role in chronic inflammation [1]. The morphological and functional expression of B_1 receptors in TG and dorsal root ganglion (DRG) neurons, however, is controversial. In DRG neurons, constitutive B_1 receptor expression, assessed immunohistochemically, has been reported [21, 22], while B_1 receptor activation-induced $[Ca^{2+}]_i$ responses have not been observed in DRG neurons [23]. Although constitutive expression of the B_1 receptor has been described in TG neurons [22], in our previous study, we were unable to observe a clear localization of B_1 receptors in cryosections prepared from intact TG tissue, although we did observe weak immunoreactivity for these receptors in primary-cultured TG neurons [3]. Interestingly, the B_1 receptor mRNA expression was barely detectable in the intact tissue; however, in primary-cultured TG neurons,

the B_1 receptor mRNA expression has been reported to depend on the length of the culture period [24]. In addition, both the results from our previous [3] and present studies clearly show that Lys-[Des-Arg^9]BK, a metabolite of endogenous BK in peripheral tissues [25], is capable of triggering $[Ca^{2+}]_i$ changes in TG neurons, in contrast to DRG neurons. These morphological and mRNA expression patterns of B_1 receptors in primary-cultured TG neurons or intact TG tissue suggest that B_1 receptor expression is induced in TG neurons as a result of tissue damage and/or inflammation. They also suggest a role for B_1 receptors in modulating nociceptive functions. Although further studies are required to determine the expression pattern of B_1 receptors in TG neurons, these neurons clearly express B_1 receptors that mobilize intracellular Ca^{2+} [1–4].

In conclusion, we have demonstrated the expression of B_1 receptors in primary-cultured TG neurons and clarified the intracellular signaling pathway that follows B_1 receptor activation. An agonist for B_1 receptors, Lys[Des-Arg^9]BK, mobilizes $[Ca^{2+}]_i$ via activation of the intracellular Ca^{2+} releasing pathway that is mediated by ryanodine receptors. The intracellular signaling pathways that increase the $[Ca^{2+}]_i$ are activated by suppression of intracellular cAMP production. Thus, the effects of B_1 receptors in TG neurons may possibly be mediated by a G_i pathway.

Acknowledgements The authors thank the Japan Society for the Promotion of Science (JSPS) Grants-in-Aid for Scientific Research (KAKENHI) and the Multidisciplinary Research Center for Jaw Disease (MRCJD) for financial support.

Author contributions RT, MK, TI, MT and YS were responsible for the conception and design of the experiments. RT, MK, AH, YK and YS were responsible for the acquisition, analysis and interpretation of data. RT, MK, TI, MT and YS were responsible for drafting and critically revising the intellectual content of the article. YS was responsible for final approval of the version to be submitted/published; All authors have read and approved the final manuscript.

Funding This research was funded by JSPS KAKENHI (grant numbers JP15K11129, JP15K11056) and by Multidisciplinary Research Center for Jaw Disease (MRCJD): Achieving Longevity and Sustainability by Comprehensive Reconstruction of Oral and Maxillofacial Functions

Compliance with ethical standards

Conflict of interest The authors declare that they have no conflict of interest.

Ethical approval All applicable international, national, and/or institutional guidelines for the care and use of animals were followed.

References

1. Leeb-Lundberg LMF, Marceau F, Müller-Esterl W, Pettibone DJ, Zuraw BL (2005) International Únion of Pharmacology. XLV. Classification of the kinin receptor family: from molecular mechanisms to pathophysiological consequences. Pharmacol Rev 57:27–77
2. Luiz AP, Schroeder SD, Rae GA, Calixto JB, Chichorro JG (2015) Contribution and interaction of kinin receptors and dynorphin A in a model of trigeminal neuropathic pain in mice. Neuroscience 300:189–200
3. Kawaguchi A, Sato M, Kimura M, Yamazaki T, Yamamoto H, Tazaki M, Ichinohe T, Shibukawa Y (2015) Functional expression of bradykinin B1 and B2 receptors in neonatal rat trigeminal ganglion neurons. Front Cell Neurosci 9:229
4. Luiz AP, Schroeder SD, Chichorro JG, Calixto JB, Zampronio AR, Rae GA (2010) Kinin B_1 and B_2 receptors contribute to orofacial heat hyperalgesia induced by infraorbital nerve constriction injury in mice and rats. Neuropeptides 44:87–92
5. Kawaguchi A, Sato M, Kimura M, Ichinohe T, Tazaki M, Shibukawa Y (2015) Expression and function of purinergic $P2Y_{12}$ receptors in rat trigeminal ganglion neurons. Neurosci Res 98:17–27
6. Shibukawa Y, Suzuki T (1997) Measurements of cytosolic free Ca^{2+} concentrations in odontoblasts. Bull Tokyo Dent Coll 38:177–185
7. Sato M, Furuya T, Kimura M, Kojima Y, Tazaki M, Sato T, Shibukawa Y (2015) Intercellular odontoblast communication via ATP mediated by pannexin-1 channel and phospholipase C-coupled receptor activation. Front Physiol 6:326
8. Tsumura M, Sobhan U, Muramatsu T, Sato M, Ichikawa H, Sahara Y, Tazaki M, Shibukawa Y (2012) TRPV1-mediated calcium signal couples with cannabinoid receptors and sodium–calcium exchangers in rat odontoblasts. Cell Calcium 52:124–136
9. Gafni J, Munsch JA, Lam TH, Catlin MC, Costa LG, Molinski TF, Pessah IN (1997) Xestospongins: potent membrane permeable blockers of the inositol 1,4,5-trisphosphate receptor. Neuron 19:723–733
10. Sato M, Ogura K, Kimura M, Nishi K, Ando M, Tazaki M, Shibukawa Y (2018) Activation of mechanosensitive transient receptor potential/piezo channels in odontoblasts generates action potentials in cocultured isolectin B_4-negative medium-sized trigeminal ganglion neurons. J Endod 44:984–991
11. Mathis SA, Criscimagna NL, Leeb-Lundberg LM (1996) B_1 and B_2 kinin receptors mediate distinct patterns of intracellular Ca^{2+} signaling in single cultured vascular smooth muscle cells. Mol Pharmacol 50:128–139
12. El-Bizri N, Bkaily G, Wang S, Jacques D, Regoli D, D'Orléans-Juste P, Sukarieh R (2003) Bradykinin induced a positive chronotropic effect via stimulation of T- and L-type calcium currents in heart cells. Can J Physiol Pharmacol 81:247–258
13. Kitakoga O, Kuba K (1993) Bradykinin-induced ion currents in cultured rat trigeminal ganglion cells. Neurosci Res 16:79–93
14. Ifuku M, Färber K, Okuno Y, Yamakawa Y, Miyamoto T, Nolte C, Merrino VF, Kita S, Iwamoto T, Komuro I, Wang B, Cheung G, Ishikawa E, Ooboshi H, Bader M, Wada K, Kettenmann H, Noda M (2007) Bradykinin-induced microglial migration mediated by B_1-bradykinin receptors depends on Ca^{2+} influx via reverse-mode activity of the Na^+/Ca^{2+} exchanger. J Neurosci 27:13065–13073
15. Kuroda H, Sobhan U, Sato M, Tsumura M, Ichinohe T, Tazaki M, Shibukawa Y (2013) Sodium–calcium exchangers in rat trigeminal ganglion neurons. Mol Pain 9:22
16. Macmillan D, McCarron JG (2010) The phospholipase C inhibitor U-73122 inhibits Ca^{2+} release from the intracellular sarcoplasmic reticulum Ca^{2+} store by inhibiting Ca^{2+} pumps in smooth muscle. Br J Pharmacol 160:1295–1301
17. De Smet P, Parys JB, Callewaert G, Weidema AF, Hill E, De Smedt H, Erneux C, Sorrentino V, Missiaen L (1999) Xestospongin C is an equally potent inhibitor of the inositol 1,4,5-trisphosphate receptor and the endoplasmic-reticulum Ca^{2+} pumps. Cell Calcium 26:9–13

18. Murthy KS, Makhlouf GM (1995) Interaction of cA-kinase and cG-kinase in mediating relaxation of dispersed smooth muscle cells. Am J Physiol 268:C171–C180
19. Nalli AD, Kumar DP, Al-Shboul O, Mahavadi S, Kuemmerle JF, Grider JR, Murthy KS (2014) Regulation of $G\beta\gamma_i$-dependent PLC-β3 activity in smooth muscle: inhibitory phosphorylation of PLC-β3 by PKA and PKG and stimulatory phosphorylation of $G\alpha_i$-GTPase-activating protein RGS2 by PKG. Cell Biochem Biophys 70:867–880
20. Hall JM (1992) Bradykinin receptors: pharmacological properties and biological roles. Pharmacol Ther 56:131–190
21. Wotherspoon G, Winter J (2000) Bradykinin B_1 receptor is constitutively expressed in the rat sensory nervous system. Neurosci Lett 294:175–178
22. Ma QP, Hill R, Sirinathsinghji D (2000) Basal expression of bradykinin B_1 receptor in peripheral sensory ganglia in the rat. NeuroReport 11:4003–4005
23. Brand M, Klusch A, Kurzai O, Valdeolmillos M, Schmidt RF, Petersen M (2001) No evidence for bradykinin B_1 receptors in rat dorsal root ganglion neurons. Neuroreport 12:3165–3168
24. Ceruti S, Villa G, Fumagalli M, Colombo L, Magni G, Zanardelli M, Fabbretti E, Verderio C, van den Maagdenberg AM, Nistri A, Abbracchio MP (2011) Calcitonin gene-related peptide-mediated enhancement of purinergic neuron/glia communication by the algogenic factor bradykinin in mouse trigeminal ganglia from wild-type and R192Q Cav2.1 Knock-in mice: implications for basic mechanisms of migraine pain. J Neurosci 31:3638–3649
25. Regoli D, Rizzi A, Perron SI, Gobeil F (2001) Classification of kinin receptors. Biol Chem 382:31–35